

Single-Source Precursor Route for the Synthesis of EuS Nanocrystals

Tihana Mirkovic, Margaret A. Hines,[†] P. Sreekumari Nair, and Gregory D. Scholes*

Lash-Miller Chemical Laboratories, University of Toronto, 80 St. George Street,
Toronto, Ontario, Canada M5S 3H6

Received November 4, 2004. Revised Manuscript Received April 1, 2005

A single-source precursor synthetic route for the preparation of colloidal EuS nanocrystals is reported. By varying the decomposition conditions of the lanthanide complex, cube-, sphere-, or polygon-shaped nanocrystals with good colloidal stability are prepared. Size control is not achieved. It is demonstrated that chelating ligands incorporated into the precursor, for example, 1,10-phenanthroline and 2,2'-bipyridine, are integrated, together with the stabilizing ligands trioctylphosphine and oleylamine, onto the nanocrystal surface.

Introduction

Inorganic nanocrystals are currently an active field of research in modern materials chemistry. There has been a large academic interest in nanocrystal systems due to the enormous range of physical properties afforded by size-tuning of these materials, which cannot be obtained from the same material in bulk. Controlling the size distribution and shape poses important challenges. Over the past decade, various solution-phase synthetic schemes for the preparation of semiconductor nanoparticles have been employed, including the most widely used organometallic synthetic procedure—high-temperature thermolysis.^{1,2} More recently, several groups have reported alternative procedures utilizing single-source precursors for the preparation of semiconductor nanoparticles.^{3–5} Here we present a single-source synthetic route for the fabrication of europium sulfide nanocrystals. We show that the shape of the final nanostructure is highly sensitive to the conditions under which precursor decomposition occurs, but the size of the colloidal particles cannot be controlled in the systematic manner familiar from other semiconductor nanocrystal preparations.

EuS is a ferromagnetic semiconductor with a Curie temperature of 16.8 K, an energy gap of 1.6 eV, and a spin splitting of the gap of 0.36 eV.^{6–8} Recently, nanocrystalline EuS has been shown to have potential as an optomagnetic and luminescent material.^{9,10} This material holds promise as

an ingredient for the fabrication of devices that can be tuned by material responses to magnetic, electrical, and optical stimuli. For example, films of EuS microcrystals have been shown to display a remarkably large Faraday effect.¹⁰ This suggests possible optoelectronic applications for EuS nanocrystals in optical isolators, optical circulators, and optical memory.

Although it was initially believed that the luminescence from these materials is very weak, Chen et al.⁹ demonstrated luminescence enhancement of EuS nanoclusters in zeolites. They successfully prepared EuS nanoclusters by solid-state diffusion of EuS into an ultrastable zeolite-Y with a supercage radius of 0.65 nm, ensuring the size of the semiconductor particles was close to the calculated exciton Bohr radius of EuS (~0.5 nm). More recently, liquid-phase synthesis of EuS nanocrystals was reported by Yanagida et al.,^{11,12} but their preparation involved harsh conditions and resulted in noncolloidal particles.

Here we report synthetic procedures to produce nanoparticles of numerous shapes varying in size from 2 to 50 nm, depending on the conditions under which the precursor decomposition takes place. Owing to the small Bohr radius of EuS, these nanoparticles do not exhibit quantum confinement in their optical properties. We synthesized EuS nanocrystals by decomposition of each of the precursors shown in Figure 1 in coordinating solvents. EuS nanocrystals prepared from the dithiocarbamate-based single-source precursors were thoroughly investigated, and it was shown that they can also include a chelating ligand that becomes bound to the nanocrystal surface. We suggest that the presence of the chelating ligand significantly influences the growth kinetics, explaining why nanocrystal size cannot be easily controlled. Here we report the incorporation of two different chelating ligands, 1,10-phenanthroline (Phen) and 2,2'-

* To whom correspondence should be addressed. E-mail: gscholes@chem.utoronto.ca.

[†] Present address: Evident Technologies, 216 River St., Troy, NY 12180.

- (1) Murray, C. B.; Norris, D. J.; Bawendi, M. G. *J. Am. Chem. Soc.* **1993**, *115*, 8706.
- (2) Qu, L.; Peng, Z. A.; Peng, X. *Nano Lett.* **2001**, *1*, 333.
- (3) Nair, P. S.; Radhakrishnan, T.; Revaprasadu, N.; Kolawole, G.; O'Brien, P. *J. Mater. Chem.* **2002**, *12*, 2722.
- (4) Lee, S.; Jun, Y.; Cho, S.; Cheon, J. *J. Am. Chem. Soc.* **2002**, *124*, 11244.
- (5) Pradhan, N.; Efrima, S. *J. Am. Chem. Soc.* **2003**, *125*, 2050.
- (6) Hao, X.; Moodera, J. S.; Meservey, R. *Phys. Rev. B* **1990**, *42*, 8235.
- (7) Eastman, D. E.; Holtzberg, F.; Methfessel, S. *Phys. Rev. Lett.* **1969**, *23*, 226.
- (8) McGuire, T. R.; Shafer, M. W. *J. Appl. Phys.* **1964**, *35*, 984.
- (9) Chen, W.; Zhang, X.; Huang, Y. *Appl. Phys. Lett.* **2000**, *76*, 2328.

- (10) Tanaka, K.; Tatehara, N.; Fujita, K.; Hirao, K. *J. Appl. Phys.* **2001**, *89*, 2213.
- (11) Thongchont, S.; Hasegawa, Y.; Wada, Y.; Yanagida, S. *J. Phys. Chem. B* **2003**, *107*, 2193–2196.
- (12) Thongchont, S.; Hasegawa, Y.; Wada, Y.; Yanagida, S. *Chem. Lett.* **2003**, *32*, 706.

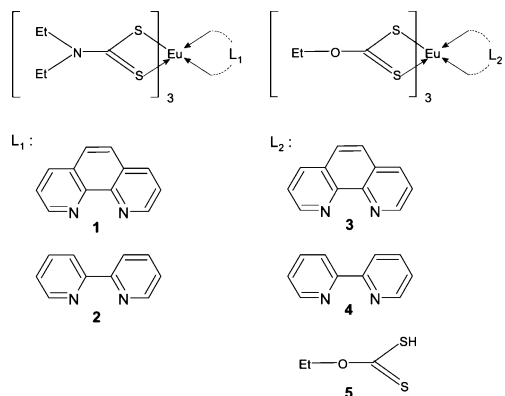


Figure 1. Europium complexes used as single-source precursors in EuS synthesis.

bipyridine (Bipy), onto the semiconductor nanoparticle surface in conjunction with the oleylamine and trioctylphosphine (TOP) stabilizing ligands from the growth solution. The surface-bound chelating ligands could be used to design functionalized supermolecular nanocrystals. Studies have shown that lanthanide complexes are highly luminescent,^{13,14} and thus, surface functionalization of the nanocrystals might be used to change the emissive properties, or may enable construction of even more elaborate supermolecular surface architectures, providing a route to coupled paramagnetic array structures.

Experimental Section

All chemicals used in the synthetic procedures of this work were purchased from Aldrich and used without further purification.

Synthesis of Eu(Ddte)₃(Phen). In the nanocrystal synthesis, a heteroligand lanthanide complex, synthesized according to a literature procedure,¹⁵ was utilized as a single-source precursor. In a typical synthesis, a solution of 1,10-phenanthroline monohydrate, Phen·H₂O (2 mmol in 20 mL of boiling water), was added to an aqueous solution of EuCl₃·6H₂O (2 mmol in 20 mL) under vigorous stirring. Dropwise addition of a sodium diethyldithiocarbamate [Na(Ddte)·H₂O] solution (9 mmol in 40 mL of water) to the above mixture resulted in a deep-orange-colored solid precipitate, which was filtered and dried in vacuo at room temperature. The yield was ~85%. The IR spectra of the complex displayed characteristic peaks from the 1,10-phenanthroline ligand at 1624, 1589, 1572, and 1516 cm⁻¹ attributed to the skeleton vibration of the benzene ring in addition to the peaks at 852 and 730 cm⁻¹ which are assigned to the bend vibration of C···CH in the complex. These peaks are shifted with respect to the peaks in the noncoordinated ligand (1617, 1587, 1561, and 1504 cm⁻¹ and 854 and 739 cm⁻¹). Additional selected frequencies (ν , cm⁻¹) used for identification were $\nu(\text{C-N}) = 1482$ cm⁻¹ and $\nu(\text{C-S}) = 1000$ cm⁻¹. The observed peaks correspond to the ones reported in refs 15 and 16, where this compound was prepared via a slightly different synthetic route.

Synthesis of Eu(Ddte)₃(Bipy). Analogous to the above-described precursor synthesis, 2,2'-bipyridine can be substituted for Phen to yield a slightly different precursor, **2**, in a 75% yield. A similar complex, Eu(Me₂dte)₃(Bipy), was reported by Su et al.,¹⁶ but their synthesis was carried out in acetonitrile. The red solid was

characterized using IR spectroscopy. The observed peaks were $\nu(\text{C-N}) = 1483$ cm⁻¹ and $\nu(\text{C-S}) = 997$ cm⁻¹, and the characteristic absorptions of 2,2'-bipyridine were found at 1594, 1566, and 771 cm⁻¹, which are in close agreement with the bands observed for the related complex from ref 16.

Synthesis of EuS Nanocubes from Eu(Ddte)₃(Phen) in TOP and Oleylamine. The heteroligand lanthanide diethyldithiocarbamate complex Eu(Ddte)₃(Phen) was subsequently used in the synthesis of the EuS semiconductor nanocrystals. In the preparation of nanocubes, 0.08 g of the dried precursor Eu(Ddte)₃(Phen) was added to 2 mL of TOP and 3 mL of oleylamine at room temperature. The resulting mixture was heated to 280 °C under argon, resulting in a purple-burgundy-colored colloidal solution. The nanocrystal growth period involved stirring of the reaction mixture at 280 °C under argon for 1 h, during which small aliquots were extracted for characterization. The nanocrystals were purified by precipitation with anhydrous methanol or ethyl acetate. The precipitate was collected by centrifugation and subsequently dispersed in toluene or heptane (Figure 2A).

Synthesis of EuS Nanodots from Eu(Ddte)₃(Phen) in TOP and Oleylamine. The alternative synthetic approach involved injection of the precursor into the growth solvent at a temperature above that necessary for thermal decomposition of the precursor. This procedure yielded sphere-shaped nanoparticles. A 3 mL portion of oleylamine was heated under vacuum at 120 °C for 30 min. The solvent was then put under argon, and the temperature was increased to 300 °C. At that point a suspension of 0.08 g of the precursor in 2 mL of TOP was injected into the reaction flask. The nanoparticles, shown in Figure 2B, were grown in an inert atmosphere at a temperature of 300 °C for 1 h.

Synthesis of EuS Nanodots from Eu(Ddte)₃(Bipy) in TOP and Oleylamine. Decomposition of 0.3 g of this lanthanide complex, Eu(Ddte)₃(Bipy), in 2 mL of TOP and 3 mL of oleylamine under argon at 200 °C for 1 h resulted in EuS nanocrystals (Figure 2C).

Synthesis of EuS Nanocrystals from Eu(Ddte)₃(Phen) in Octadecene, Oleylamine, and Oleic Acid. A series of syntheses were performed using a solvent mixture composed of octadecene, oleic acid, and oleylamine. In a typical synthesis a mixture of 0.3 g of Eu(Ddte)₃(Phen) in 2.7 mL of octadecene, 1 mL of oleic acid, and 1.7 mL of oleylamine was heated under vacuum at 100 °C for 30 min. Subsequently, the mixture was put under argon and heated at 300 °C for 1 h. The resulting nanoparticles are shown in Figure 2D. A similar protocol was adopted for the synthesis of EuS nanoparticles in Figure 2E, where the solvent mixture was composed of 2.7 mL of octadecene and 2.7 mL of oleylamine.

Xanthate Precursors. Both dithio/selenocarbamates and xanthates have previously been used as precursors for the synthesis of II–VI semiconductor nanoparticles.¹⁷ Xanthates, which have coordinating sites similar to those of dithiocarbamates, were also explored as a sulfur source in the preparation of EuS nanocrystals. The xanthate-based precursors **3–5** were sufficiently stable to isolate and characterize;^{18,19} nonetheless, we found that better quality nanoparticles were synthesized from precursors generated in situ as described below.

Synthesis of Eu(EtOCS₂)₃(Phen). A solution of potassium ethyl xanthate (0.48 g, 3 mmol) and 1,10-phenanthroline (0.198 g, 1 mmol) in 20 mL of 2-propanol was added to europium chloride

(13) Kurata, S.; Nagai, M. *Anal. Sci.* **2002**, *19*, 451.

(14) Maas, H.; Currao, A.; Calzaferri G. *Angew. Chem., Int. Ed.* **2002**, *41*, 2495.

(15) Ivanov, R. A.; Korsakov, I. E.; Formanovskii, A. A.; Paramonov, S. E.; Kuz'mina, N. P.; Kaul', A. R. *Russ. J. Coord. Chem.* **2002**, *28*, 670.

(16) Su, C.; Tan, M.; Tang, N.; Gan, X.; Liu, W. *J. Coord. Chem.* **1996**, *38*, 207.

(17) Malik, A.; Revaprasadu, N.; O'Brien, P. *Chem. Mater.* **2001**, *13*, 913.

(18) Savost'yanova, A. F.; Skopenko, V. V.; Rakhlin, M. Ya.; Sukhan, T. A. *Dokl. Akad. Nauk Ukr. SSR, Ser. B: Geol., Khim. Biol. Nauki* **1989**, *1*, 49.

(19) Savost'yanova, A. F.; Khavryuchenko, V. D. *Russ. J. Inorg. Chem.* **1994**, *39*, 1742.

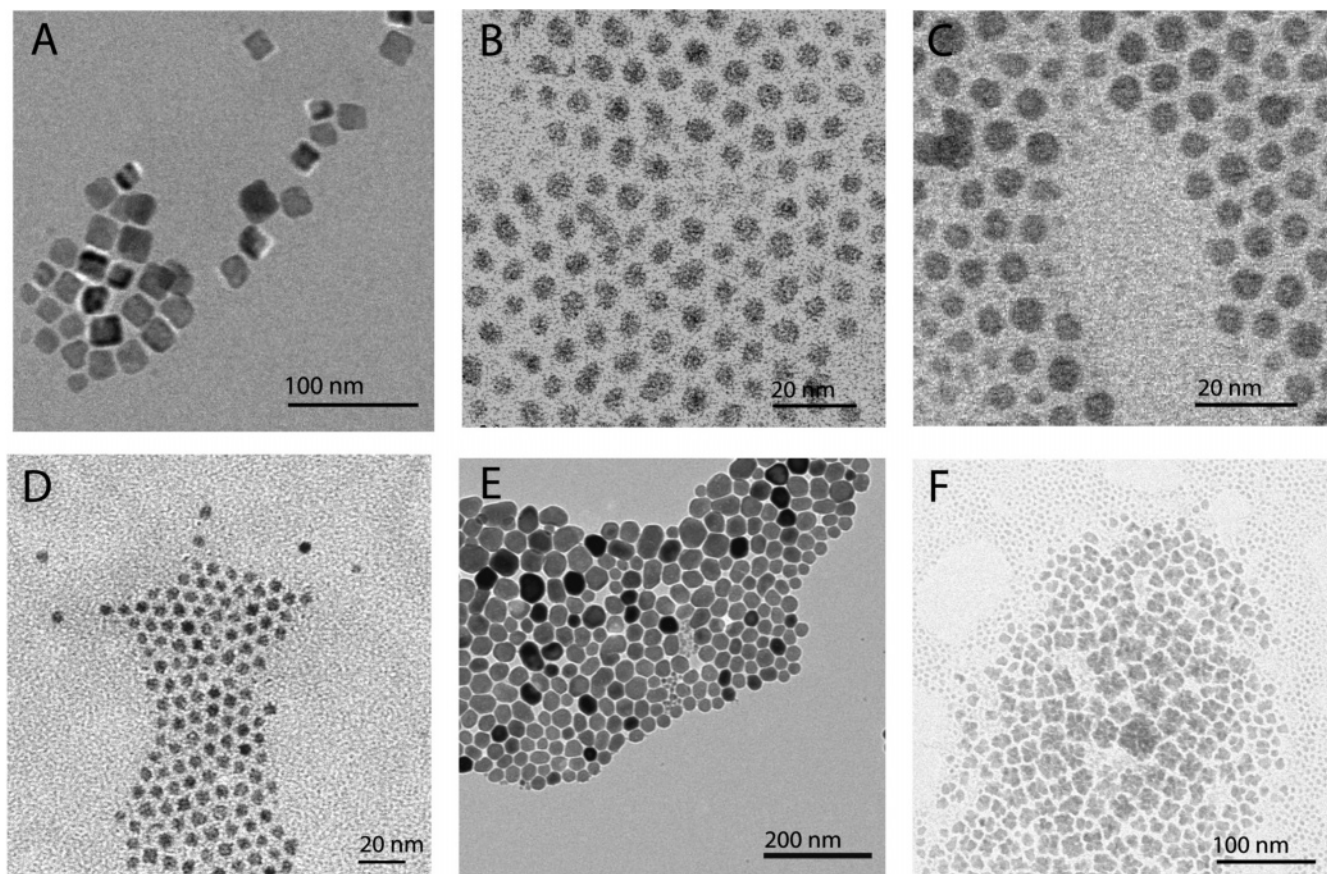


Figure 2. TEM images of EuS nanocrystals: (A) cubes synthesized by heating precursor **1** to 280 °C in TOP and oleylamine; (B) dots prepared by injection of precursor **1** into TOP and oleylamine at 300 °C; (C) EuS dots obtained by heating precursor **2** in TOP and oleylamine to 200 °C; (D) nanodots obtained through the decomposition of precursor **1** in a mixture of octadecene, oleylamine, and oleic acid at 300 °C; (E) truncated-polyhedral nanoparticles synthesized from precursor **1** at 300 °C using a solvent mixture of octadecene and oleylamine; (F) nanocrystal aggregates.

(0.26 g, 1 mmol) in 15 mL of 2-propanol. The mixture was refluxed for 2 h. The solution on cooling gave a pale pink solid, which was filtered and washed with 2-propanol and dried. The yield was ~82%. IR (KBr, cm^{-1}): $\nu_{(\text{OC})}$ = 1463 (m), $\nu_{(\text{CS})_{\text{as}}}$ = 1182 (m), $\nu_{(\text{CC})}$ = 1133 (s), ν_{CSsy} = 810 (m), Phen peaks, skeletal vibrations of the benzene ring, at 1617, 1587, 1561, and 1504. Anal. Calcd for $\text{EuC}_{21}\text{H}_{23}\text{O}_3\text{N}_2\text{S}_6$: C, 36.26; H, 3.31; N, 4.03. Found: C, 36.43; H, 3.03; N, 4.19.

Synthesis of $\text{Eu}(\text{EtOCS}_2)_3(\text{Bipy})$. A solution of potassium ethyl xanthate (0.48 g, 3 mmol) and 2,2'-bipyridyl (0.16 g, 1 mmol) in 20 mL of 2-propanol was added to europium chloride (0.26 g, 1 mmol) in 15 mL of 2-propanol. The mixture was refluxed for 2 h. The solution on cooling gave a pale pink solid, which was filtered and washed with 2-propanol and dried. The yield was ~74%. IR (KBr cm^{-1}): $\nu_{(\text{OC})}$ = 1463 (m), $\nu_{(\text{CS})_{\text{as}}}$ = 1180 (m), $\nu_{(\text{CC})}$ = 1135 (s), $\nu_{(\text{CS})_{\text{sy}}}$ = 804 (m). Anal. Calcd for $\text{EuC}_{19}\text{H}_{23}\text{O}_3\text{N}_2\text{S}_6$: C, 33.98; H, 3.43; N, 4.17. Found: C, 34.13; H, 3.29; N, 4.14.

Synthesis of $\text{KEu}(\text{EtOCS}_2)_4$. Employing a variation of the procedure from the one reported in ref 17, this precursor was prepared by adding a solution of potassium ethyl xanthate (0.64 g, 4 mmol) in 15 mL of 2-propanol to europium chloride (0.26 g, 1 mmol) in 15 mL of 2-propanol. The mixture was refluxed for 2 h. The solution on cooling gave a solid, which was filtered and washed with 2-propanol and dried. The yield was 80%. IR (KBr cm^{-1}): $\nu_{(\text{OC})}$ = 1462 (m), $\nu_{(\text{CS})_{\text{as}}}$ = 1180 (m), $\nu_{(\text{CC})}$ = 1137 (s), ν_{CSsy} = 815 (m). The IR data correspond well to the bands reported in ref 19.

Synthesis of EuS Nanocrystals from Xanthate-Based Precursors. The ethyl xanthate potassium salt and europium chloride were dispersed in TOP, and upon being stirred for 45 min under argon,

the dispersion was injected into oleylamine at room temperature and heated at 315 °C for 1 h. The nanocrystals prepared in this fashion were of lower quality than their diethyldithiocarbamate counterparts.

Characterization. Transmission electron microscopy (TEM) images were recorded using a TEI Technai 20 instrument equipped with a Gatan camera. Powder X-ray diffraction (PXRD) measurements were carried out on a Siemens D5000 diffractometer using a high-power $\text{Cu K}\alpha$ source operating at 50 kV and 35 mA with a Kevex solid-state detector. A step scan mode was used for data collection with a step size of 0.02 deg and time of 2.0 s per step. Absorption spectra were obtained on a CARY 100 BIO UV-vis spectrophotometer. Infrared spectra were measured in the range 400–4000 cm^{-1} as pressed pellets in KBr on a Perkin-Elmer Spectrum 1000 FT-IR spectrophotometer.

Results and Discussion

Arriving at the desired shape and size of nanocrystals requires a delicate balance and control of various reaction parameters. Nucleating seeds, kinetic control, temperature, and selective modulation of activation energies for crystal growth planes through the use of capping molecules are crucial for anisotropic growth.²⁰ Examples of previous work on designing shape-guiding strategies for the production of nanocrystals include work on CdSe rods,^{21–23} where growth

(20) Lee, S.; Cho, S.; Cheon, J. *Adv. Mater.* **2003**, *15*, No. 5, 441.

(21) Peng, X.; Manna, L.; Yang, W.; Wickham, J.; Scher, E.; Kadavanich, A.; Alivisatos, A. P. *Nature* **2000**, *404*, 59.

is directed parallel to the inherently anisotropic (*c*-axis) of its hexagonal cell structure. Some work on Pt nanocrystals²⁴ has shown that shapes, including cubes and tetrahedra, can be prepared. Lee et al. have demonstrated a series of shape evolutions ranging from anisotropic (i.e., rods) to isotropic (i.e., cubes) forms even in rock salt phase semiconductors, such as lead sulfide.⁴ O'Brien and co-workers have reported shape control of CdS nanocrystals related to the chemical nature of the single-source precursor.²⁵

In a number of cases it has been observed that the tunability of the synthesis and shape control is further complicated by the presence of impurities, which tend to adsorb on the surface of the nanocrystals, suppressing their growth. Those observations were initially made by Reinders,²⁶ who noticed that, in the presence of a small amount of methylene blue, the AgCl crystals grew to an irregular dendritic shape instead of the ordinary symmetrical one. More recently, Yang et al.²⁷ reported a similar finding, where correct conformation of their surface ligand, ethylenediamine, was crucial in obtaining nanocrystals of a desired shape. A similar experiment using *o*-phenanthroline as the surface binding agent yielded irregularly shaped particles, suggesting that the binding properties of surface ligands are critical to the final shape of the nanocrystal. In addition to shape control, it was shown by Marc et al.²⁸ that the presence of additives, such as quinoline yellow, during crystallization of potassium sulfate can have a profound effect on the kinetics of crystal growth. Additionally, at high enough concentration of the impurity, it was demonstrated that the crystallization process could be entirely stopped. We believe that, in our system, the bidentate ligands, such as 1,10-phenanthroline or 2,2'-bipyridine, act as impurities and might considerably influence the crystallization process of europium sulfide. For example, we have discovered that small changes in the decomposition conditions of the lanthanide precursor have a large effect on the final shape of the EuS nanocrystals. That can be explained as an interplay between the kinetics of EuS growth with adsorption and slow desorption kinetics of the Phen or Bipy.

Figure 2 displays TEM images of the different EuS nanoparticles obtained following the synthetic procedures in this study. The nature of the decomposition of this lanthanide precursor seems to be dependent on its chemical environment in addition to the thermal conditions; thus, tuning and controlling the nanocrystal growth process presented a true challenge. The high sensitivity of the decomposition process of the EuS precursor leads to a variation in nucleation and growth kinetics, ultimately resulting in the formation of nanocrystals in various shapes and sizes. Analogous to PbS, EuS has a rock salt structure and it is expected that the

precursor decomposition is followed by the formation of tetradecahedron seeds which are terminated by {100} and {111} faces.²⁰ A number of different decomposition conditions yielded nearly spherical nanoparticles shown in Figure 2B–D. These nanocrystals are all 5–7 nm in size, whereas the nanocrystals that exhibit a cubic or polygonal morphology (Figure 2A,E) tend to be larger, 20–50 nm. This transition from smaller spherical nanoparticles to larger faceted nanocrystals has been observed by other researchers.²⁴ It is believed that, for small nanocrystals, which have a very large surface:volume ratio, the lowest energy can be achieved through surface minimization. This is accomplished when the small nanocrystals adopt a spherical morphology. However, as the size of the nanocrystal increases, decreasing the fraction of atoms on the surface, the morphology of the particles becomes more dependent on the surface energies of the specific crystalline faces. In addition, the presence of capping molecules can selectively lower the surface energy of one face relative to another, leading to the formation of nanocrystals of variant morphologies, depending on the solvent composition.

In a rock salt system, the surface energy of the {111} faces is typically high, and in the presence of weakly binding capping molecules at high temperature, the formation of cube-shaped nanocrystals is favored.²⁰ However, in the presence of tightly binding ligands that coordinate preferentially to the {111} faces, polygon-shaped nanocrystals which are highly truncated on the {111} faces are formed.²⁰ Similar arguments may apply to the formation of cubic and polygonal nanoparticles of EuS (Figure 2A,E). It is hard to speculate about the energetics of specific crystal faces under the different synthetic conditions given the presence of unknown intermediates during the precursor decomposition, which might be able to bind to the surface and have a significant influence on the final nanocrystal morphology. The situation is further complicated by the diverse range of coordinating ligands available for binding to the crystals during growth. These include Phen, Bipy, oleylamine, and TOP.

An additional observation made for this single-source reaction system is the formation of "cubic" aggregates for a number of conditions that were investigated. A variation in the synthesis of nanocubes shown in Figure 2A yielded a hierarchy of coagulated particles (Figure 2F). The phenomena could be explained by insufficient surface passivation, leading to aggregate formation. Similar aggregates were observed for iron oxide by Redl et al.³⁰

A number of known systems can be tuned through a variation of one reaction parameter. In the preparation of iron oxide nanoparticles Teng³¹ et al. have shown how manipulation of the oleic acid concentration can dramatically improve the monodispersity of their nanocrystals. Our synthetic routes rely on oleylamine, an alkylamine, which is shown to promote the decomposition, and also acts as a

(22) Manna, L.; Scher, E.; Alivisatos, A. P. *J. Am. Chem. Soc.* **2000**, *122*, 12700.

(23) Peng, Z. A.; Peng, X. *J. Am. Chem. Soc.* **2002**, *124*, 3343.

(24) Ahmadi, T. S.; Wang, Z. L.; Green, T. C.; Henglein, A.; El-Sayed, M. A. *Science* **1996**, *272*, 1924.

(25) Nair, P. S.; Radhakrishnan, T.; Revaprasadu, N.; Kolawole, G. A.; O'Brien P. *Chem. Commun.* **2002**, *6*, 564.

(26) Reinders, W. *Z. Phys. Chem.* **1911**, *77*, 677.

(27) Yang, J.; Zeng, J.; Yu, S.; Yang, L.; Zhou, G.; Qian, Y. *Chem. Mater.* **2000**, *12*, 3259–3263.

(28) Marc, R.; Wenk, W. *Z. Phys. Chem.* **1910**, *68*, 104.

(29) Joo, J.; Na, H.; Yu, T.; Yu, J.; Kim, Y.; Wu, F.; Zhang, J.; Hyeon, T. *J. Am. Chem. Soc.* **2003**, *125*, 11100.

(30) Redl, F. X.; Black, C. T.; Papaefthymiou, G. C.; Sandstrom, R. L.; Yin, M.; Zeng, H.; Murray, C. B.; O'Brien, S. P. *J. Am. Chem. Soc.* **2004**, *126*, 14583.

(31) Teng, X.; Yang, H. *J. Mater. Chem.* **2004**, *14*, 774.

stabilizing agent for the particles that form.³² Pradhan et al.³² have demonstrated preparation of metal sulfide nanoparticles using a xanthate-based precursor and employing an alkylamine Lewis base solvent. They reported that analogously prepared nanocrystals using dithiocarbamates in the synthesis were of lower quality compared to their xanthate counterparts. The difference was attributed to the higher decomposition temperature of dithiocarbamate precursors, conditions under which fabrication of high-quality nanoparticles becomes less feasible. Our system faces similar challenges as the thermal decomposition of the lanthanide dithiocarbamate precursor occurs at 290 °C. Additionally, the interdependence of the reaction parameters in our system makes fine-tuning of the shape and size of the EuS nanocrystals through systematic variation of reaction conditions less feasible. The presence of chelating ligands incorporated into the precursor, 1,10-phenanthroline and 2,2'-bipyridine, adds to the complexity of the reaction system, as those ligands might be competing with oleylamine for surface sites on the nanocrystals. Yang et al.²⁷ have shown that adsorption of 1,10-phenanthroline on the surface of CdS leads to the formation of irregularly shaped particles. This is likely to be a reason for the low reproducibility and poor size and shape control of the EuS nanocrystals.

Examination of the corresponding PXRD patterns of the nanocubes revealed that they have a cubic rock salt crystal structure, characteristic of bulk EuS (Figure 3A). The conventional value for the intensity ratio of the (200) to the (111) diffraction peak is significantly smaller than that observed here. This is because the nanocubes tended to self-organize so that their {100} planes were preferentially oriented parallel to the surface of the supporting substrate. The fairly narrow peak widths suggest a high structural quality of the sample. An even higher crystallinity was observed for a faceted nanocrystal sample (Figure 3B).

The absorption spectrum of the lanthanide precursor dissolved in a 1:1 mixture of methanol and toluene shows a prominent peak at 435 nm that is attributed to the ligand to metal charge transfer. UV-vis absorption spectra of both the EuS cubes and dots prepared from Eu(Dtc)₃(Phen) in TOP and oleylamine showed a dominant peak centered at ~500 nm, Figure 4A. Analogous to other semiconductor nanocrystals, one would expect the dominant absorption feature in the visible to be attributed to the quantum-confined lowest exciton transition. However, that band, Figure 4A, did not exhibit a size-dependent shift for any sample we prepared and furthermore is not evident in bulk EuS. The lack of quantum confinement is expected, as all the nanocrystals prepared in this study are much larger than the predicted EuS Bohr exciton radius of ~0.5 nm.⁹ An absorption band at this energy was not exhibited by the EuS nanocrystals prepared in liquid ammonia.¹¹ Their observations suggest that the band may be related to the surface ligands. There is source literature concerning Eu²⁺ coordination compounds. An analogous absorption feature is not shown by a scandium-Phen complex, which makes it unlikely to be a metal-ligand charge-transfer (MLCT) band involving Phen.³³

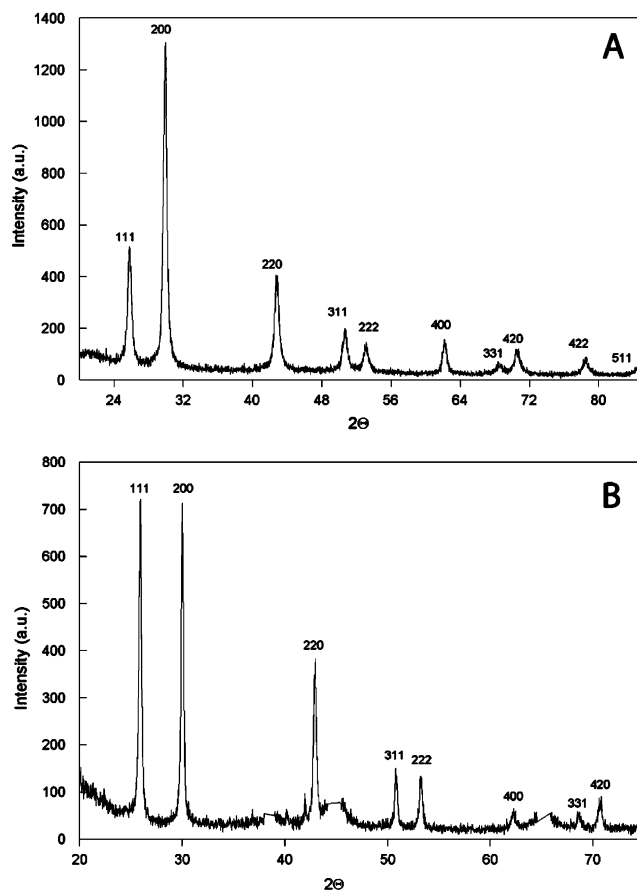


Figure 3. (A) Powder X-ray diffraction pattern of the cubic nanoparticles, confirming the rock salt (FCC) structure of EuS. (B) Powder X-ray diffraction pattern of the faceted nanoparticles showing the high crystallinity of the sample. The sharp lines around 38.5°, 44.8°, and 65.1° coming from the aluminum substrate were omitted in the figure.

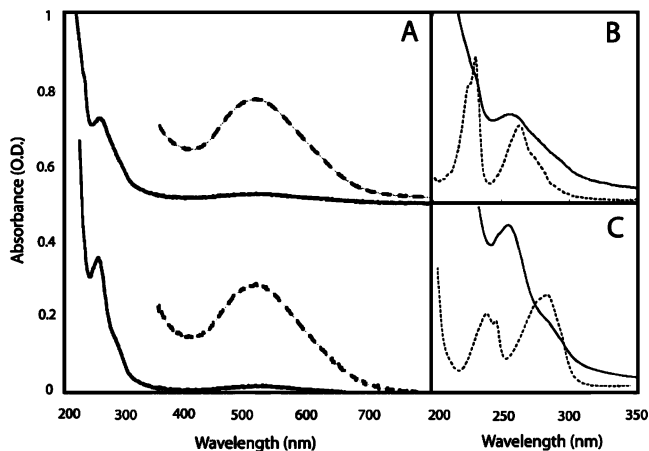


Figure 4. (A) Comparison of absorption spectra of EuS nanocrystals prepared using precursor 1 (top curves) and precursor 2 (bottom curves). The prominent feature in the visible region (attributed to MLCT) is shown for solutions of higher OD as dotted lines. (B) Absorption spectra in the UV region of nanocrystals prepared from 1 (solid line) and Phen in heptane (dotted line). (C) Absorption spectra in the UV region of nanocrystals prepared from 2 (solid line) and Bipy in heptane (dotted line).

It was not possible to test this band for solvatochromism, since the nanocrystals decomposed in more polar solvents, such as tetrahydrofuran, and liberated a trivalent europium complex that was discernible by its characteristic lumines-

(32) Pradhan, N.; Katz, B.; Efrima, S. *J. Phys. Chem. B* **2003**, *107*, 13843.

(33) Melson, G. A.; Stotz, R. W. *Coord. Chem. Rev.* **1971**, *7*, 133.

cence. However, considering previous reports of the spectroscopy of divalent europium compounds^{34–39} coordinated to, for example, unsaturated nitrogen donor ligands, it is likely that the 500 nm EuS absorption band relates to a europium $4f^7 \rightarrow 4f^65d^1$ transition. The band is shifted to lower energy because in EuS the chemical bonding delocalizes the 4f orbitals, as has been suggested by computational studies⁴⁰ and analysis of high-resolution sulfur K-edge X-ray absorption near-edge structure spectra.⁴¹ The nature of this band, such that its shape and position are independent of the environment, is characteristic of lanthanide transitions which are insensitive to the surroundings due to the shielding of 4f orbitals by the filled 5s and 5p levels.

An additional feature of the nanocrystal absorption spectrum is the high optical density (OD) in the UV region, which is attributed to the $\pi-\pi^*$ transition of the chelating ligand. Figure 4B displays a comparison of the absorption of Phen in heptane, a solvent that is essentially transparent at wavelengths >200 nm, to that when it is coordinated to the EuS nanocrystals. The same is shown for the Bipy sample in Figure 4C. It is hard to assign the bands of the nanocrystal samples that are observed in the high-energy region, but it is expected that, due to the change in the environment, the chelating ligands would have a different absorption in the free floating form compared to when they are coordinated to the surface of EuS nanocrystals. In contrast to the transition observed at 500 nm, which is common to both the EuS samples prepared from precursors **1** and **2**, the absorption spectra of the two EuS samples show distinctly different features in the UV region, suggesting that the origin of those bands is attributed to the coordinating ligands, rather than the nanocrystalline EuS. Coordination of ligands such as 1,10-phenanthroline and 2,2'-bipyridine to the surface of nanocrystals has been previously observed by other authors.^{27,42} This observation, the presence of bidentate ligands on the surface of the nanocrystals, further strengthens our theory that coordination of 1,10-phenanthroline or 2,2'-

bipyridine during crystal growth might have a large effect on the tunability of the crystallization process of EuS nanoparticles.

Conclusion

We have utilized a single-source precursor synthetic route for preparation of colloidal EuS nanocrystals. It was found that, by varying the decomposition conditions of the lanthanide precursor complex, nanocrystals of varying shapes and sizes could be obtained. The nature of the decomposition was such that fine-tuning of the size or shape of the nanocrystals was not achievable. It is believed that the presence of chelating ligands, left over upon precursor decomposition, interfere with the crystal growth of the nanoparticles, reducing the reproducibility and the quality of the nanocrystals. A spherical-to-cubic transition in the shape of the nanocrystals was observed as they increased in size. It was noted that a number of reaction conditions resulted in the production of spheres in the 5–8 nm size regime. On the contrary, cubic and faceted-polyhedral nanostructures were always in the size range of 20–50 nm. We reported the incorporation of two different chelating ligands, Phen and Bipy, onto the semiconductor nanoparticle surface in conjunction with the oleylamine and TOP stabilizing ligands from the growth solution. UV–vis analysis of the nanocrystal samples suggests that the surface of these nanostructures incorporates a significant number of bound Phen or Bipy. The chelating ligands were important for stabilizing the single-source precursor, which also provided the Eu^{2+} and S^{2-} . A positive outlook suggests that integration of organic functionality with these inorganic nanocrystals opens up possibilities for the controlled, directed assembly of the EuS nanocrystals into arrays.⁴³ This capability may enable engineering of elaborate multicomponent “metamaterials” that incorporate magnetic, optical, and electrical functionality and interfacing.⁴⁴

Acknowledgment. The Natural Sciences and Engineering Research Council of Canada is gratefully acknowledged for financial support. M.A.H. thanks Dr. P. Mulvaney for valuable discussions. G.D.S. is an A. P. Sloan fellow.

Supporting Information Available: IR and UV–vis spectra of $\text{Eu}(\text{Ddtc})_3(\text{Phen})$, $\text{Eu}(\text{Ddtc})_3(\text{Bipy})$, $\text{KEu}(\text{OCS}_2)_3(\text{Phen})$, $\text{KEu}(\text{OCS}_2)_3(\text{Bipy})$, and $\text{KEu}(\text{OCS}_2)_4$ (PDF). This material is available free of charge via the Internet at <http://pubs.acs.org>.

CM048064M

(34) Shipley, C. P.; Capecechi, S.; Salata, O. V.; Etchells, M.; Dobson, P. J.; Christou, V. *Adv. Mater.* **1999**, *11*, 533.

(35) Jiang, J.; Higashiyama, N.; Machida, K.; Adachi, G. *Coord. Chem. Rev.* **1998**, *170*, 1.

(36) Berardini, M.; Brennan, J. *Inorg. Chem.* **1995**, *34*, 6179.

(37) Berardini, M.; Emge, T.; Brennan, J. G. *J. Am. Chem. Soc.* **1993**, *115*, 8501.

(38) Mikheev, N. B.; Kamenskaya, A. N. *Coord. Chem. Rev.* **1991**, *109*, 1.

(39) Liu, W.; Hong, G.; Dai, D.; Li, L.; Dolg, M. *Theor. Chem. Acc.* **1997**, *96*, 75.

(40) Rogalev, A.; Goulon, J.; Brouder, C. *J. Phys.: Condens. Matter* **1999**, *11*, 1115.

(41) Alpha, B.; Lehn, J.-M.; Mathis, G. *Angew. Chem., Int. Ed. Engl.* **1987**, *26*, 266.

(42) Deng, H.; Li, M.; Yu, Z.; Lu, Z.; Fu, D. *Chem. Lett.* **1997**, *6*, 483.

(43) Balzani, V.; Scandola, F. *Supramolecular Photochemistry*; Ellis Horwood: Chichester, U.K., 1991.

(44) Redl, F. X.; Cho, K. S.; Murray, C. B.; O'Brien, S. *Nature* **2003**, *423*, 968.